drones

MDPI

Article

Mapping Stratigraphy and Artifact Distribution with Unmanned Aerial Vehicle-Based Three-Dimensional Models—A Case Study from the Post Research Area in Northwestern Texas, USA

Stance Hurst [1,2,*], Eileen Johnson [1,2,*] and Doug Cunningham [2]

[1] Heritage and Museum Sciences, Museum of Texas Tech University, 3301 4th St, Lubbock, TX 79415, USA
[2] Lubbock Lake Landmark, 2401 Landmark Drive, Lubbock, TX 79415, USA; douglas.cunningham@ttu.edu
* Correspondence: stance.hurst@ttu.edu (S.H.); eileen.johnson@ttu.edu (E.J.)

Abstract: This study applies UAV-based photogrammetry to map and examine the stratigraphy and archaeological artifact distribution in two localities within the Post research area in northwest Texas. A DJI Inspire 1 UAV equipped with a Zenmuse X5 camera captured nadir and oblique images. These were processed using Agisoft Metashape to generate 3D models. These models enabled the precise mapping of stratigraphic boundaries, revealing the distinctions between Triassic-age bedrock, Pleistocene-age alluvial deposits, and Holocene-age aeolian sediments. Field surveys from 2022 to 2024 documented over 5000 artifacts with sub-centimeter accuracy, including diagnostic projectile points and ceramics. This research highlights the advantages of UAV-derived 3D models in rapidly and accurately documenting stratigraphy and archaeological data. It demonstrates the value of UAV technology for visualizing landscape-scale processes and artifact contexts, offering a new approach to understanding the interactions between geomorphology and archaeology. The findings contribute to advancing UAV applications in both geomorphological and archaeological research.

Keywords: unmanned aerial vehicles (UAVs); photogrammetry; 3D visualization; stratigraphy

Citation: Hurst, S.; Johnson, E.; Cunningham, D. Mapping Stratigraphy and Artifact Distribution with Unmanned Aerial Vehicle-Based Three-Dimensional Models—A Case Study from the Post Research Area in Northwestern Texas, USA. *Drones* **2024**, *8*, 684. https://doi.org/10.3390/drones8110684

Academic Editors: Giordano Teza, Massimo Fabris, Arianna Pesci and Tina Živec

Received: 30 September 2024
Revised: 6 November 2024
Accepted: 15 November 2024
Published: 19 November 2024

1. Introduction

Using Unmanned Aerial Vehicles (UAVs) in geological and archaeological research has revolutionized landscape documentation, analysis, and interpretation [1,2]. UAVs are widely used in structural geology for mapping complex formations, identifying fault structures, and analyzing earthquake coseismic ruptures [3]. In sedimentary geology, they help analyze depositional environments [4] and are also employed to monitor rock mass fractures and natural hazards, such as landslides and rockfalls [5]. In archaeology, UAVs facilitate the documentation of sites and the creation of detailed 3D models, enhancing the mapping and visualization of cultural features and surface artifacts across various environments while deepening our understanding of past human activity [6]. The ability to construct high-resolution 3D models from aerial imagery in particular has enhanced the understanding of stratigraphic relationships and geomorphological processes in various contexts [7–10].

Most UAV studies have focused primarily on the plan-view mapping of landscapes [11,12], which provides valuable information about surface features but often lacks the depth needed for stratigraphic analysis. In contrast, this study emphasizes the use of oblique imagery [9,10,13,14], which captures cross-sectional views of the landscape, allowing for a detailed examination of stratigraphy across a study area.

One key motivation for this research is to explore the potential of UAV photogrammetry in developing 3D models for stratigraphic mapping. This process can be conducted more quickly and accurately than traditional field-based techniques [3,8,15]. Software tools such as VRGeoscience (https://www.vrgeoscience.com/ accessed on 25 October 2024) have demonstrated the value of 3D visualization, providing a powerful means to document

and analyze geological outcrops in a three-dimensional context [16]. In this study, Agisoft Metashape (https://www.agisoft.com/ accessed on 25 October 2024) software is employed to achieve similar objectives, leveraging its capabilities to create detailed 3D models that accurately represent stratigraphic sequences.

Despite the significant advancements made through UAV technology and photogrammetry software, a gap remains in the literature concerning integrating UAV-derived data with detailed stratigraphic and archaeological survey analyses. This gap is particularly noticeable in regions where complex interactions between geomorphological processes and human activity exist. Previous studies have often focused on either geomorphology or archaeology independently [2,7,11,17–20], with few exploring the nuanced relationships between these two domains within a unified framework.

This study addresses this gap by applying UAV photogrammetry to localities within the Post research area in northwestern Texas, integrating high-resolution 3D models with stratigraphic mapping and surface artifact distribution analysis. By doing so, this research provides detailed documentation of the region's geological and archaeological features and offers insights into how these elements interact across the landscape.

2. Materials and Methods

2.1. Post Research Area

The Post research area (Figures 1 and 2) is located at the physiographic boundary between the Southern High Plains and the Rolling Plains (Central Lowlands). The Southern High Plains extend across northwestern Texas and northeastern New Mexico, while the Rolling Plains lie immediately to the east (Figure 1). The Southern High Plains are defined by escarpments on three sides, with the southern boundary merging seamlessly with the Edwards Plateau without a distinct division. Characterized as a broad, flat plateau, the upland surfaces of the Southern High Plains encompass approximately 25,000 small lake basins (freshwater playas) and 40 salinas (saline depressions with brackish water) [21]. The region is dissected by northwest-to-southeast-trending river valleys (draws) that serve as tributaries to the Red, Brazos, and Colorado Rivers, which ultimately drain into the Gulf of Mexico.

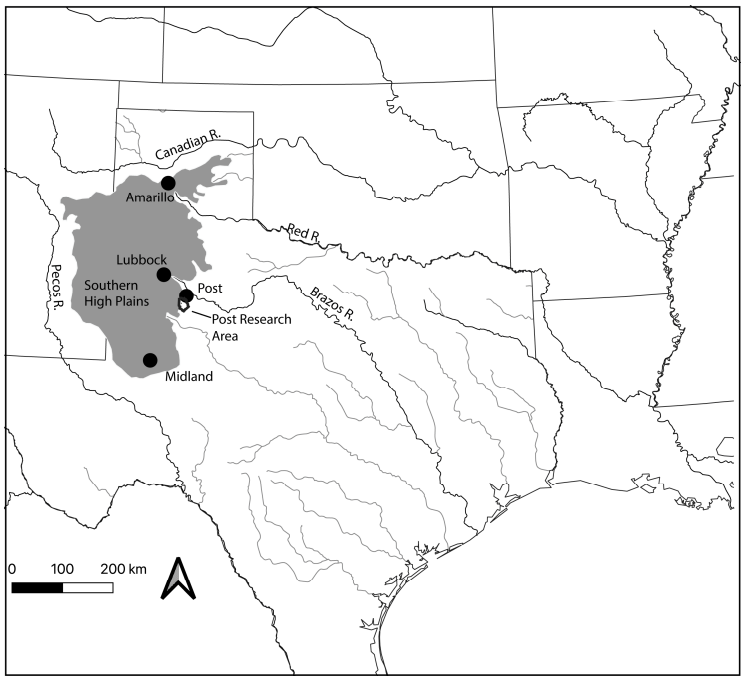

Figure 1. The Southern High Plains of northwestern Texas and eastern New Mexico (USA). The Post research area is situated along the eastern escarpment, extending into the westernmost portion of the Rolling Plains of Texas.

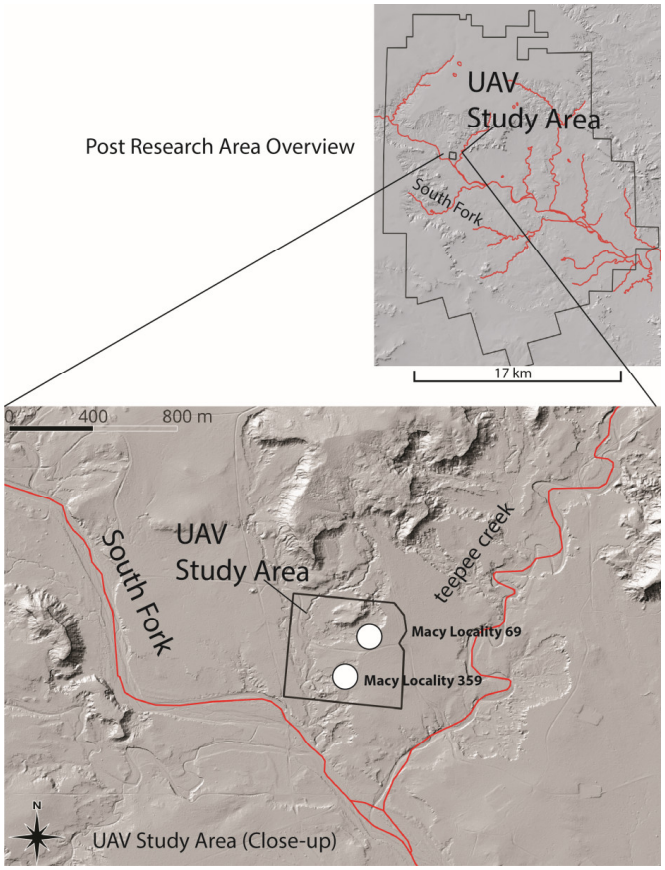

Figure 2. The Post research area and the location of the UAV study area along the South Fork.

During the Pleistocene, headward erosion along the eastern escarpment of the Southern High Plains selectively exposed Triassic-age mudstones, sandstones, and conglomerates of the Dockum Group [22], along with the gravels, aeolian sediments, and Caprock caliche layer that make up the Miocene-to-Pliocene-age Ogallala Formation within the research area [23]. Unlike the flat expanse of the Southern High Plains, the area below the eastern escarpment is characterized by rough, broken terrain—referred to as the "breaks"—formed through the incision and erosion of the differentially resistant sediments of the Ogallala Formation and the underlying Triassic sandstone bedrock [22,24]. Within the research area, these breaks are dissected by numerous tributaries of the upper Brazos River Basin.

The Post research area comprises ~335 km^2 of ranchland, encompassing portions of the Southern High Plains uplands, escarpment breaks, and the westernmost Rolling Plains. The South Fork of the Double Mountain Fork of the Brazos River (hereafter South Fork) flows from northwest to southeast through the research area (Figure 2) with numerous spring-fed tributaries. These tributaries, serving as the primary conduits for water discharge, play a crucial role in shaping the landscape and exposing soil and stratigraphic sequences throughout the South Fork Basin. The current research focuses on a 718 × 236 m (7.6 ha) section along Teepee Creek—a tributary north of the South Fork (Figure 2).

2.2. UAV Study Locality

The UAV study area (23.6 ha) encompasses two previously documented archaeological localities within the Post research area: Macy Locality 359 (identified in 2022) and Macy Locality 69 (discovered in 2008). The UAV study locality has undergone significant erosion, revealing the stratigraphy over a distance of 2.7 km (Figure 3). This erosion and substantial archaeological surface findings offer a unique opportunity to document the contextual relationships between the artifacts, landscape, and stratigraphy of this area.

Figure 3. Erosional surface and exposed stratigraphy at Macy Locality 69, documented in 2024 in the Post research area. View to the west.

The local bedrock of the UAV study area consists of the Triassic Dockum Group that underlies the Quaternary stratigraphic sequence [22]. The Dockum Group is exposed at the surface in erosional zones in the study area, characterized primarily by Triassic overbank mudstone. In some locations, the sandstone layer that caps the mudstone remains preserved [25].

Unconformably overlying the Triassic mudstone are stratified Pleistocene-age alluvial deposits and Holocene aeolian sand deposits. The precise age of the Pleistocene alluvial deposits remains undetermined. Mammoth bone found at the top of the alluvial sequence (Figure 4) indicates a middle-to-late Pleistocene (Irvingtonian to Rancholabrean) age [26]. The Holocene-age aeolian sand deposit rests unconformably on the alluvial and Triassic bedrock within the study area.

Figure 4. Stratigraphic units and the location of mammoth bone within alluvium at Macy Locality 359. View to the southeast.

The absence of buried soils within this deposit indicates continuous sedimentation, preventing the formation of a stable, steady-state surface necessary for the formation of buried soils [27]. The diagnostic lithic artifacts associated with the aeolian deposits suggest

that deposition began ~6000 years ago in this location. Elsewhere, along the South Fork and within the Spring Creek drainage, a sequence of buried soils within the Holocene aeolian deposits have been radiocarbon-dated to between ~6000 and 300 ^{14}C yr B.P. [28–30]. Ongoing research, including the excavation of hearth features and continued surveys to identify additional in situ diagnostic artifacts, aims to refine further the age of the aeolian deposits within the UAV study area.

2.3. Survey Techniques

2.3.1. UAV Stratigraphic Mapping

A DJI Inspire 1 UAV equipped with a 16-megapixel (4600 × 2584) Zenmuse X5 camera was used to capture a total of 1453 images over 10 flights, consisting of 1005 nadir images (69%) and 448 (31%) oblique images (Figure 5). A plano-altimetric survey at a constant height of 50 m above ground level was used to capture all nadir images. In contrast, the oblique images were captured at variable distances between 30 and 15 m above ground following the terrain. The focus of the oblique image capture was to obtain close-up images of erosional cuts, ensuring highly detailed surface imagery with sufficient texture resolution for stratigraphic mapping. The UAV was manually controlled, with images overlapping between 30 and 60% (Figure 6).

Figure 5. Capturing oblique images with DJI Inspire 1 UAV in the Post research area. View to the west.

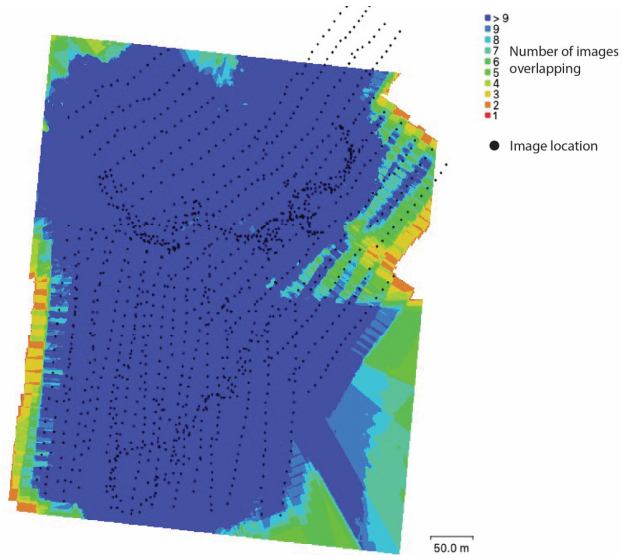

Figure 6. Camera location and image overlap of the UAV study area in the Post research area. Figure generated from Agisoft Metashape survey statistics report.

2.3.2. Archaeological Survey

Field crew members mapped and collected archaeological artifacts throughout the UAV study area during the 2022, 2023, and 2024 field seasons (Figure 7A). All surface artifacts were mapped and collected using a Trimble R8 integrated GNSS system with centimeter accuracy. Of the 5143 artifacts documented and collected, most consisted of flaked stone—the byproducts of stone tool manufacture or maintenance. Five in situ hearth features were also recorded along the eroded edge (Figure 7B).

Figure 7. (**A**) Field research at Macy Locality 359 within the UAV study area. (**A**) Crew mapping and collecting archaeological artifacts using the Trimble R8 base station. View to the south. (**B**) Field crew documenting hearth feature eroding from the top of the aeolian deposit. View to the south.

Thirty-one diagnostics were found throughout the study area: twenty-eight projectile points and three ceramic sherds (Figure 8). The styles of the projectile points and ceramic sherds provide an approximate age range of 6000–350 years ago for both the prehistoric occupations and the aeolian deposit.

Figure 8. Projectile points and ceramic sherd found at Macy Locality 359 and Macy Locality 69 during the 2022–2024 field seasons. (**A**) Middle Archaic-age projectile point (6000–4500 BP); (**B**–**F**) Late Archaic-age projectile points (4500–2000 BP); (**G**–**H**) Ceramic-age projectile points (2000–500 BP); (**I**) ceramic sherd (575–350 BP).

2.4. Photogrammetry and Data Visualization

The images were imported into Agisoft Metashape 2.1.2 for photogrammetric processing using a 2022 Apple Macbook Pro with an M2 Max Processor consisting of 12 CPU and 30 GPU cores. All 1453 images were aligned successfully, yielding 774,463 tie points and achieving a ground resolution of 0.0315 mm/pixel. The model was then georeferenced using five natural ground control points recorded with a Trimble R8 base station. This

georeferencing process resulted in a model accuracy of X error at 2.19 cm, Y error at 2.07 cm, and Z error at 4.36 cm, with an overall horizontal (XY) error of 3.01 cm and a total error of 4.86 cm.

A tiled model, DEM, and orthomosaic of the UAV survey area were constructed in the second phase of the analysis. The tiled model achieved a 2.33 cm/pixel resolution, allowing for a highly detailed 3D representation of the landscape. The DEM provided a point density of 0.169 points/cm^2 and a resolution of 2.43 cm/pixel, offering a precise digital elevation profile for terrain analysis. The orthomosaic was constructed at a 1.22 cm/pixel resolution, ensuring a high-resolution, georeferenced 2D map of the area.

In the final step, the stratigraphic boundaries across the UAV study area were digitized within the tile model using Metashape's polyline tool. The stratigraphic boundaries were mapped along vertical cross-section erosional cuts across the study area. Additionally, the 5143 artifacts, the locations of the hearth features, and the mammoth bone were imported into Metashape as a point shapefile for visualization.

3. Results

3.1. Stratigraphic Mapping

The high-resolution tile model facilitated detailed mapping of the stratigraphic boundaries across the UAV study area (Figure 9). The erosional surface and the boundaries between the Triassic bedrock, alluvial, and aeolian sediment units were visible (Figure 9). Also, distinct layers within the alluvial sediments were observed throughout the study area (Figure 9).

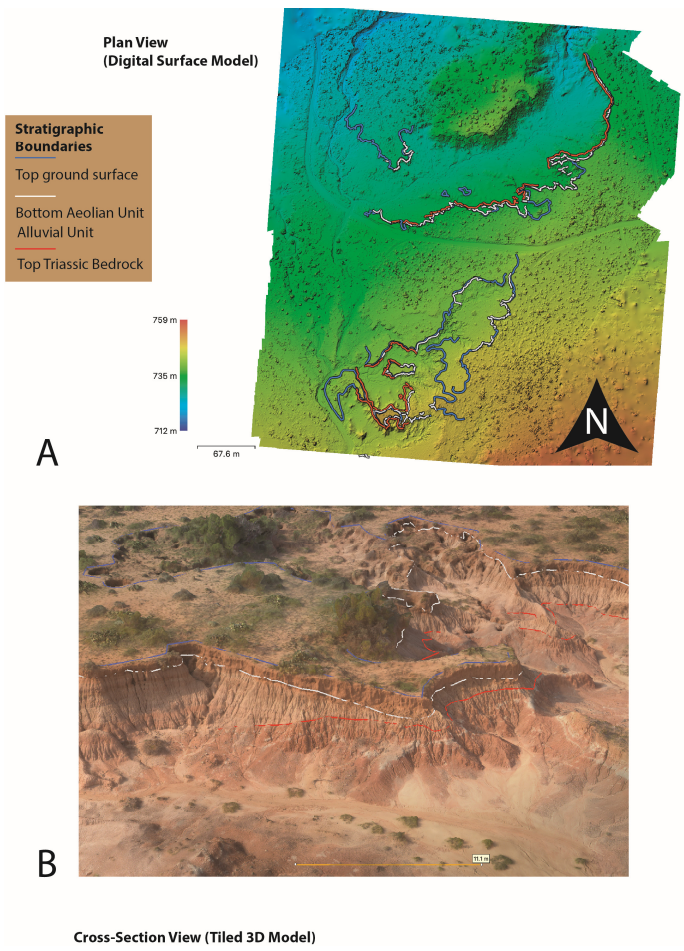

Figure 9. View of stratigraphic units within the 3D tile model of the UAV study area. View to the southeast. (**A**) Plan view of the distribution of stratigraphic boundaries, (**B**) Stratigraphic units mapped across 3D model. Yellow line demarcates scale in meters.

The top of the ground surface was initially mapped over a distance of 2723 m (Figure 9) to establish the total length of stratigraphy that could be mapped across the study area. Subsequently, the lower boundary of the aeolian unit was mapped over a distance of 1743 m. The aeolian sediment, which forms the top layer, covers 64% of the landscape in the study area.

The aeolian unit is distinguishable from the alluvial unit and Triassic bedrock by its color and erosion patterns, which are visible within the 3D model. The aeolian unit is browner (10YR4/3) than the alluvial unit (2.5YR 6/2–5/4). It exhibits a vertical 90-degree slope due to its subangular blocky soil structure, contrasting with the other two units (Figure 10). The aeolian unit is mapped above the alluvial unit throughout most of the study area. In a 30 m erosional section, however, the alluvial unit has been removed by previous erosion, resulting in the aeolian unit being mapped directly atop the Triassic Dockum Group (Figure 11).

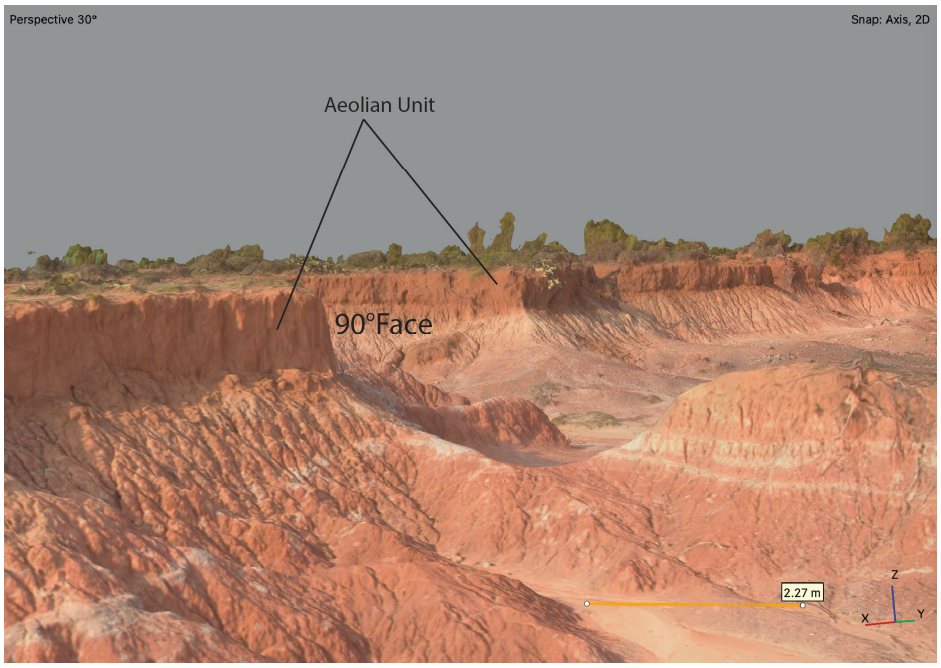

Figure 10. Three-dimensional view (tile model) of the 90° erosional face of the aeolian unit across the UAV study area, illustrating the distinct vertical exposure of stratigraphy. View to the south. Yellow line demarcates scale in meters.

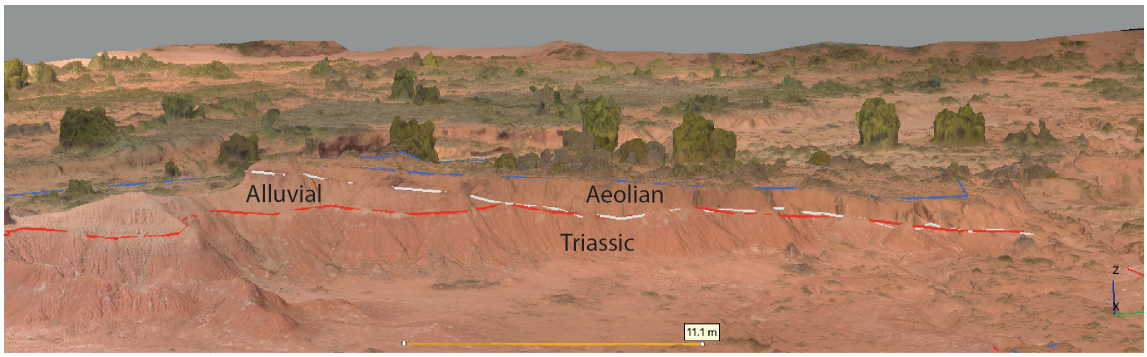

Figure 11. Three-dimensional view (tile model) of the aeolian unit and its unconformable boundary above the Triassic Dockum Group in the UAV study area. View to the west. Yellow line demarcates scale in meters.

The alluvial unit's lower and upper boundaries are plotted over 2403 m. This length indicates that the alluvial stratigraphic unit is present across 87.9% of the landscape. The alluvial sediment has become cemented with other elements, resulting in columnar structure with slopes ranging from 80 to 60 degrees (Figure 12). The alluvial unit is also lighter gray (2.5YR6/2) than the aeolian sediment.

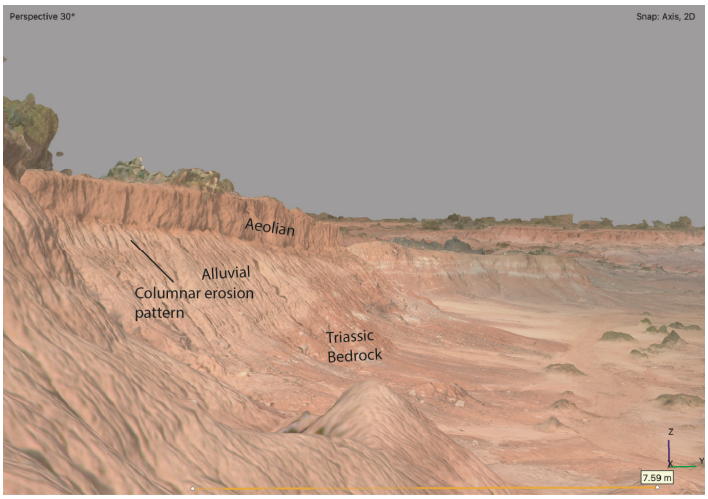

Figure 12. Three-dimensional view (tile model) of the columnar erosional pattern of the alluvial unit in the UAV study area. View to the west. Yellow line demarcates scale in meters.

The top of the Triassic Dockum Group was mapped over a distance of 947 m, making it visible in the cross-section across 34% of the study area. The Triassic bedrock, characterized by its distinct red color (10R4/8), stands out compared to the other stratigraphic units. Within the 3D model, the topographic influence of the Triassic bedrock and the subsequent deposition of alluvial sediments are distinct. In several locations across the study area, the top of the Triassic bedrock is higher in the landscape. It forms a lateral boundary to the deposition of the alluvial unit. Within the 3D model, the Triassic bedrock's topographic influence and the alluvial sediments' subsequent deposition are clearly distinguishable (Figure 13).

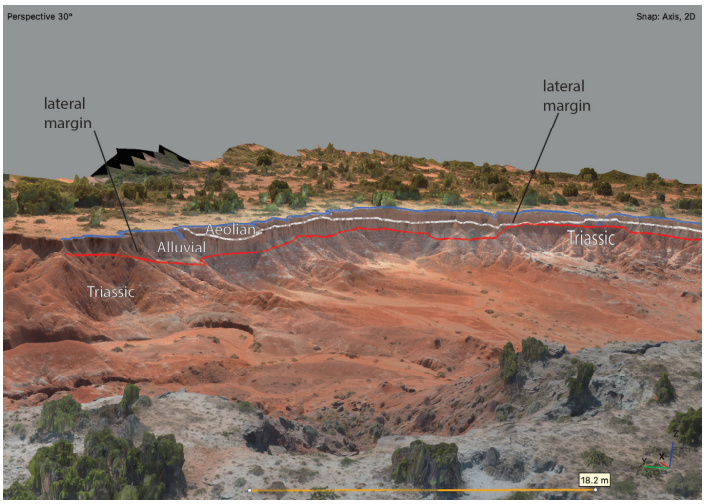

Figure 13. Three-dimensional view (tile model) of the Triassic Dockum Group bedrock. The distinct red color (10R4/8) of the Triassic bedrock contrasts with other stratigraphic units, showing its topographic influence and forming a lateral boundary to the deposition of alluvial sediments. View to the south. Yellow line demarcates scale in meters.

3.2. Visualization of Stratigraphy and Archaeology

The field crew's mapping of artifact locations and features was imported as a shapefile into Metashape and plotted on the tile model (Figure 14). This integration of the tile model, stratigraphy mapping, and artifact locations offers a clear visual representation of how artifacts are distributed across the landscape in relation to the stratigraphy. Viewing the artifact distribution within a 3D model, as opposed to traditional GIS, allows for a more intuitive interpretation of the spatial patterns and the underlying processes influencing artifact placement. Linear artifact distributions, commonly attributed to the transect-based documentation of crew members, are contextualized more clearly in the 3D model. The model shows how landscape erosion and hydrological processes contribute to artifact movement and exposure. For instance, certain linear artifact clusters within the model align with slope dynamics and water flow, which likely transported artifacts downslope along erosion channels and natural water pathways [31–33] (Figure 15).

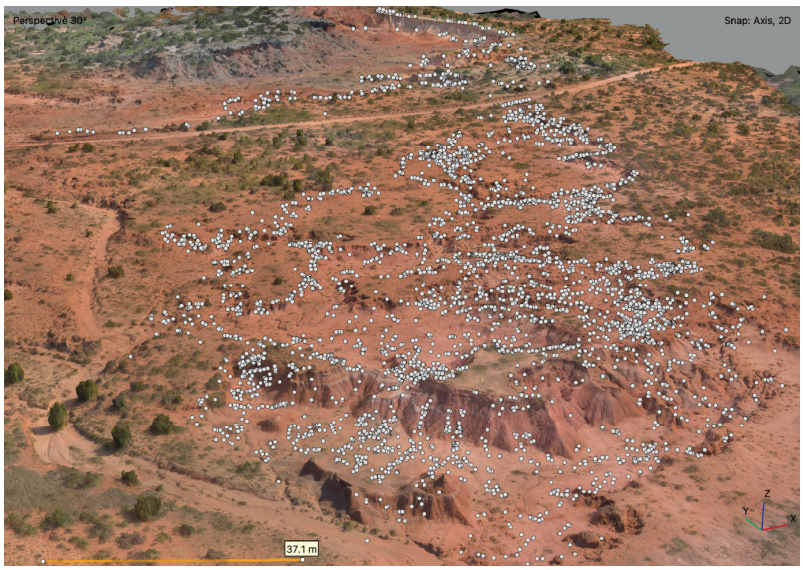

Figure 14. Overall distribution of artifacts (white points) across the UAV study area, visualized on the 3D tile model. View to the east. Yellow line demarcates scale in meters.

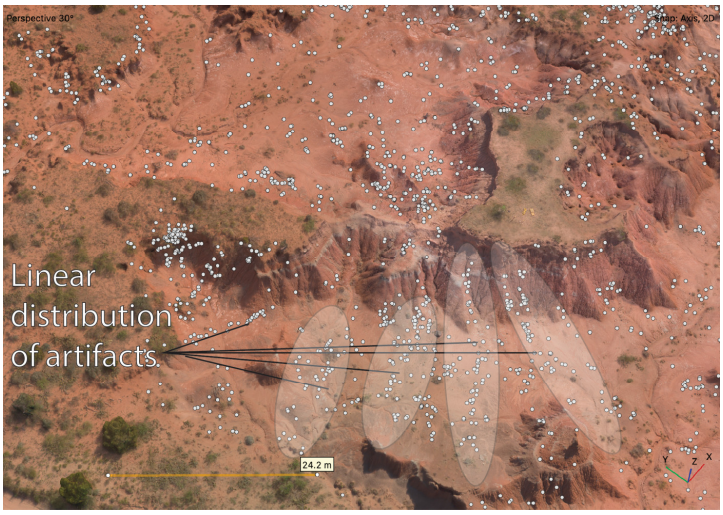

Figure 15. Linear distribution of artifacts (white points) influenced by slope and water flow, visualized on the 3D tile model, highlighting the impact of geomorphological processes on artifact dispersal. View to the east. Yellow line demarcates scale in meters.

Another key point is that the 3D model, in conjunction with the artifact data, establishes a clear contextual connection between the artifacts, stratigraphy, and the landscape. This means that the location of artifacts can be revisited in the future, allowing the contexts of artifact discoveries to be understood in their original landscape setting (Figure 16). The 3D model documents and preserves the contextual relationship between the artifacts and the landscape, a critical aspect in interpreting the past.

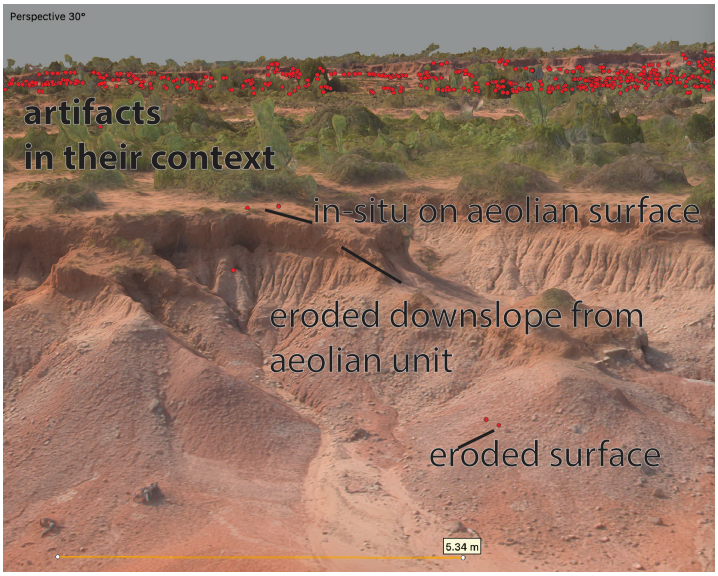

Figure 16. Visualization of artifacts (red points) within their stratigraphic context. View to the west. Yellow line demarcates scale in meters.

Additionally, the distribution of the aeolian unit across the landscape is critical in this research. This sediment layer contains artifacts from hunter-gatherer groups living on the landscape for ~6000 years. The 3D model provides a visual representation of the aeolian sediments, offering insights into how the erosion of this deposit affects artifact distribution and where archaeological materials may be preserved within the landscape (Figure 17).

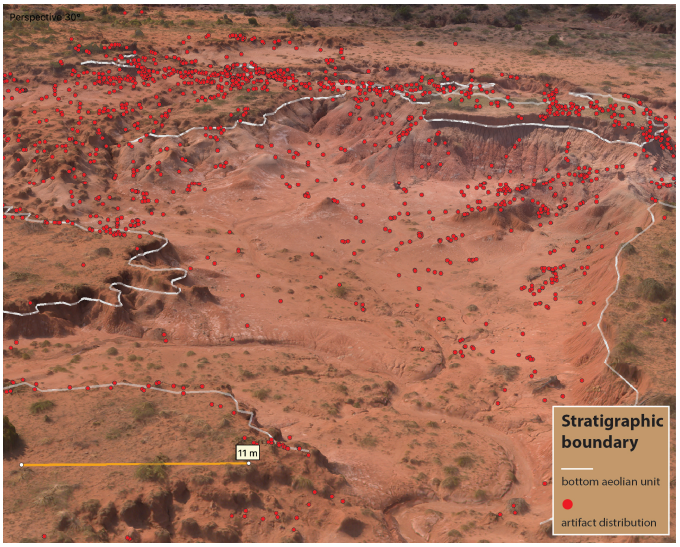

Figure 17. Visualization of the distribution of the aeolian sediment unit in relation to the distribution of artifacts across the UAV study area, using the 3D tiled model in Metashape. View to the south. Yellow line demarcates scale in meters.

4. Discussion

Integrating UAV-based photogrammetry and GNSS data in the Post research area has provided a transformative approach to understanding the landscape, stratigraphy, and artifact distribution within this archaeologically significant region. The high-resolution 3D model generated from UAV imagery has allowed for the detailed mapping of stratigraphic boundaries and provided a new level of clarity in visualizing the relationship between geological frameworks and archaeological records.

One of the key outcomes of this research is the ability to observe and analyze the distribution of artifacts in direct relation to the landscape's stratigraphic context. Traditional GIS techniques, while useful, often lack the capacity to visualize artifacts within their full 3D landscape context. The use of a 3D model in this study has highlighted the importance of considering topographic and erosional processes in interpreting artifact locations. The linear distribution patterns of artifacts, for example, clearly demonstrate the influence of slope processes and water flow in moving and exposing these materials. This insight underscores the dynamic nature of the landscape and its direct impact on the preservation and visibility of archaeological materials.

Furthermore, the 3D model has proven invaluable in documenting the stratigraphic relationships within the study area. The distinct boundaries between the Triassic bedrock, alluvial sediments, and aeolian deposits are visible, allowing for a more nuanced understanding of the region's depositional history. The aeolian unit, containing artifacts from hunter-gatherer groups dating back approximately 6000 years, is particularly significant. Visualizing this layer and its erosion patterns has provided critical information on where archaeological materials will likely be preserved or exposed, guiding future survey and excavation efforts.

The contextualization of artifacts within the 3D model also provides a lasting record that preserves the spatial relationships between artifacts, stratigraphy, and the landscape. This capability is crucial for ongoing and future research, as it allows researchers to revisit and reanalyze the context of discoveries with a level of detail that would not be possible with traditional methods. Preserving this contextual information is vital for accurate interpretation and a comprehensive understanding of the region's geomorphic processes, archaeological records, landscape evolution and use, and cultural history.

Overall, the integration of UAV technology, photogrammetry, and GIS in this study has advanced the ability to document and analyze the complex interactions between human activity and the landscape over time. The results of this research not only enhance the understanding of the Post research area, but also demonstrate the broader applicability of these techniques in archaeological studies across diverse environments. As technology continues to evolve, the methods used in this study will likely become standard practice, offering new possibilities for discovery and interpretation.

Future advancements in UAV technology promise improvements for more efficient data capture. Current limitations primarily revolve around flight time constraints, such as frequent landings for battery changes that reduce the efficiency of data capture. With anticipated improvements in UAV weight reduction and battery longevity, these interruptions may become less significant, allowing for more prolonged flights and, consequently, greater spatial coverage per session.

Additionally, automating UAV flights can enhance efficiency, especially with predefined flight paths—a method commonly used among UAV pilots for systematic data collection. This automation increases the number of images captured in each flight and ensures uniform overlap, essential for creating high-resolution, accurate models [34,35]. Although this study relied on manual flight to navigate potential unknown obstacles, automated flights now are more feasible due to obstacle detection and avoidance system advancements [36]. These capabilities allow UAVs to fly closer to the ground safely, capturing higher-resolution images and even detecting small features, and could provide valuable contextual data [37], allowing the mapping of surface artifacts in archaeological research [38,39].

5. Conclusions

This study demonstrates the powerful capabilities of UAV-based photogrammetry in archaeological and geomorphological research, particularly for detailed stratigraphic mapping and visualizing artifact distributions. The use of oblique imagery and 3D modeling allowed for the precise documentation of the stratigraphy across the study area, offering insights into the distribution of the Triassic bedrock, Pleistocene alluvial deposits, and Holocene aeolian sediments. The high-resolution 3D model created from the UAV imagery clarifies how erosion and water movement have shaped the landscape and influenced the spatial distribution of artifacts.

Furthermore, the ability to visualize these stratigraphic relationships and artifact locations within a 3D context provides a significant improvement over traditional 2D GIS methods. By preserving the spatial relationships between artifacts and stratigraphy, this approach enhances the interpretation of archaeological sites and offers a lasting record for future reanalysis.

This research not only fills a gap in the existing literature by integrating geomorphological and archaeological perspectives, but also highlights the efficiency and accuracy of UAV technology in mapping complex landscapes. As UAV and photogrammetry technology evolves, its application will become standard practice in archaeological and geological research, providing new opportunities for documenting and understanding the dynamic interactions between landscapes and human activity. This study serves as a model for utilizing UAV technology to bridge the gap between geomorphological processes and archaeological interpretations, ultimately contributing to the broader understanding of past human–landscape interactions.

Author Contributions: Conceptualization, S.H., E.J. and D.C.; methodology, S.H.; software, S.H.; validation, S.H., E.J. and D.C.; formal analysis, S.H.; investigation, S.H., E.J. and D.C.; resources, E.J.; data curation, S.H. and E.J.; writing—original draft preparation, S.H.; writing—review and editing, E.J. and S.H.; visualization, S.H.; supervision, E.J. and S.H.; project administration, E.J. All authors have read and agreed to the published version of the manuscript.

Funding: This research received no external funding.

Data Availability Statement: All data are housed at the Museum of Texas Tech University.

Acknowledgments: The authors thank the landowners for graciously allowing us access to the ranch. The manuscript represents part of the ongoing Lubbock Lake Landmark regional research into Late Quaternary landscape development and climatic and ecological change on the Southern Plains.

Conflicts of Interest: The authors declare no conflicts of interest.

References

1. Pavlis, T.L.; Mason, K.A. The New World of 3D Geologic Mapping. *GSA Today* **2017**, *27*, 4–10. [CrossRef]
2. Jorayev, G.; Wehr, K.; Benito-Calvo, A.; Njau, J.; de la Torre, I. Imaging and photogrammetry models of Olduvai Gorge (Tanzania) by Unmanned Aerial Vehicles: A high-resolution digital database for research and conservation of Early Stone Age sites. *J. Archaeol. Sci.* **2016**, *75*, 40–56. [CrossRef]
3. Bemis, S.P.; Micklethwaite, S.; Turner, D.; James, M.R.; Akciz, S.; Thiele, S.T.; Bangash, H.A. Ground-based and UAV-Based photogrammetry: A multi-scale, high-resolution mapping tool for structural geology and paleoseismology. *J. Struct. Geol.* **2014**, *69*, 163–178. [CrossRef]
4. Harrald, J.E.G.; Coe, A.L.; Thomas, R.M.; Hoggett, M. Use of drones to analyse sedimentary successions exposed in the foreshore. *Proc. Geol. Assoc.* **2021**, *132*, 253–268. [CrossRef]
5. Cirillo, D.; Zappa, M.; Tangari, A.C.; Brozzetti, F.; Ietto, F. Rockfall Analysis from UAV-Based Photogrammetry and 3D Models of a Cliff Area. *Drones* **2024**, *8*, 31. [CrossRef]
6. Hill, A.C. Economical drone mapping for archaeology: Comparisons of efficiency and accuracy. *J. Archaeol. Sci. Rep.* **2019**, *24*, 80–91. [CrossRef]
7. Whitford, B.; Boyadzhiev, K.; Ivanov, M.; Tyufekchiev, K.; Boyadzhiev, Y. A Photogrammetry-Assisted Methodology for the Documentation of Complex Stratigraphic Relationships. *Adv. Archaeol. Pract.* **2022**, *10*, 428–439. [CrossRef]
8. Chen, J.; Wang, B.; Wang, F.; Hou, M.; Hu, Z. Identification of outcropping strata from UAV oblique photogrammetric data using a spatial case-based reasoning model. *Int. J. Appl. Earth Obs. Geoinf.* **2021**, *103*, 102450. [CrossRef]

9. Chesley, J.T.; Leier, A.L.; White, S.; Torres, R. Using unmanned aerial vehicles and structure-from-motion photogrammetry to characterize sedimentary outcrops: An example from the Morrison Formation, Utah, USA. *Sediment. Geol.* **2017**, *354*, 1–8. [CrossRef]
10. Nakamura, T.; Kioka, A.; Egawa, K.; Ishii, T.; Yamada, Y. Estimating millimeter-scale surface roughness of rock outcrops using drone-flyover structure-from-motion (SfM) photogrammetry by applying machine learning model. *Earth Sci. Inform.* **2024**, *17*, 2399–2416. [CrossRef]
11. Orsini, C.; Benozzi, E.; Williams, V.; Rossi, P.; Mancini, F. UAV Photogrammetry and GIS Interpretations of Extended Archaeological Contexts: The Case of Tacuil in the Calchaqui Area (Argentina). *Drones* **2022**, *6*, 31. [CrossRef]
12. Koutalakis, P.; Tzoraki, O.; Gkiatas, G.; Zaimes, G.N. Using UAV to Capture and Record Torrent Bed and Banks, Flood Debris, and Riparian Areas. *Drones* **2020**, *4*, 77. [CrossRef]
13. Hao, J.N.; Zhang, X.L.; Wang, C.T.; Wang, H.; Wang, H.B. Application of UAV Digital Photogrammetry in Geological Investigation and Stability Evaluation of High-Steep Mine Rock Slope. *Drones* **2023**, *7*, 198. [CrossRef]
14. Honarmand, M.; Shahriari, H. Geological Mapping Using Drone-Based Photogrammetry: An Application for Exploration of Vein-Type Cu Mineralization. *Minerals* **2021**, *11*, 585. [CrossRef]
15. Quamar, M.M.; Al-Ramadan, B.; Khan, K.; Shafiullah, M.; El Ferik, S. Advancements and Applications of Drone-Integrated Geographic Information System Technology—A Review. *Remote Sens.* **2023**, *15*, 39. [CrossRef]
16. Bilmes, A.; D'Elia, L.; Lopez, L.; Richiano, S.; Varela, A.; Alvarez, M.d.P.; Bucher, J.; Eymard, I.; Muravchik, M.; Franzese, J.; et al. Digital outcrop modelling using "structure-from- motion" photogrammetry: Acquisition strategies, validation and interpretations to different sedimentary environments. *J. S. Am. Earth Sci.* **2019**, *96*, 102325. [CrossRef]
17. Vavulin, M.V.; Chugunov, K.V.; Zaitceva, O.V.; Vodyasov, E.V.; Pushkarev, A.A. UAV-based photogrammetry: Assessing the application potential and effectiveness for archaeological monitoring and surveying in the research on the 'valley of the kings' (Tuva, Russia). *Digit. Appl. Archaeol. Cult. Herit.* **2021**, *20*, e00172. [CrossRef]
18. Smith, S.L. Drones over the "Black Desert": The Advantages of Rotary-Wing UAVs for Complementing Archaeological Fieldwork in the Hard-to-Access Landscapes of Preservation of North-Eastern Jordan. *Geosciences* **2020**, *10*, 426. [CrossRef]
19. Megarry, W.; Graham, C.; Gilhooly, B.; O'Neill, B.; Sands, R.; Nyland, A.; Cooney, G. Debitage and Drones: Classifying and Characterising Neolithic Stone Tool Production in the Shetland Islands Using High Resolution Unmanned Aerial Vehicle Imagery. *Drones* **2018**, *2*, 12. [CrossRef]
20. Liu, B.L.; Coulthard, T.J. Mapping the interactions between rivers and sand dunes: Implications for fluvial and aeolian geomorphology. *Geomorphology* **2015**, *231*, 246–257. [CrossRef]
21. Sabin, T.J.; Holliday, V.T. Playas and lunettes on the Southern High Plains: Morphometric and spatial relationships. *Ann. Assoc. Am. Geogr.* **1995**, *85*, 286–305. [CrossRef]
22. Lehman, T.; Chatterjee, S. Depositional Setting and Vertebrate Biostratigraphy of the Triassic Dockum Group of Texas. *J. Earth Syst. Sci.* **2005**, *114*, 325–351. [CrossRef]
23. Gustavson, T.C.; Winkler, D.A. Depositional facies of the Miocene-Pliocene Ogallala Formation, northwestern Texas and eastern New Mexico. *Geology* **1988**, *16*, 203–206. [CrossRef]
24. Ferring, C.R. Archaeological Geology of the Southern Plains. In *Archaeological Geology of North America*; Lasca, N.P., Donahue, J., Eds.; Geological Society of America: Boulder, CO, USA, 1990; pp. 253–266.
25. Martz, J. Lithostratigraphy, Chemostratigraphy, and Vertebrate Biostratigraphy of the Dockum Group (Upper Triassic), of Southern Garza County, West Texas. Ph.D. Dissertation, Texas Tech University, Lubbock, TX, USA, 2008.
26. Bell, C., Jr.; Lundelius, E.L.; Barnosky, A.D.; Graham, R.W.; Lindsay, E.H., Jr.; Ruez, D.R., Jr.; Semken, H.A.; Webb, D.; Zakrzewski, R. The Blancan, Irvingtonian, and Rancholabrean Mammal Ages. In *Late Cretaceous and Cenozoic Mammals of North America*; Woodburne, M.O., Ed.; Columbia Press: New York, NY, USA, 2004; pp. 232–314.
27. Birkeland, P.W. *Soils and Geomorphology*, 3rd ed.; Oxford University Press: New York, NY, USA, 1999.
28. Johnson, E.; Hurst, S.; Moretti, J.A. Late Quaternary Stratigraphy and Geochronology of the Spring Creek Drainage along the Southern High Plains Eastern Escarpment, Northwest Texas. *Quaternary* **2021**, *4*, 19. [CrossRef]
29. Conley, T.; Hurst, S.; Johnson, E. Topographic Thresholds and Soil Preservation along the Southern High Plains Eastern Escarpment, Northwest Texas, USA. *Geosciences* **2020**, *10*, 476. [CrossRef]
30. Murphy, L.R.; Hurst, S.C.; Holliday, V.T.; Johnson, E. Late Quaternary Landscape Evolution, Soil Stratigraphy, and Geoarchaeology of the Caprock Canyonlands, Northwest Texas, USA. *Quat. Int.* **2014**, *342*, 57–72. [CrossRef]
31. Petraglia, M.D.; Potts, R. Water Flow and the Formation of Early Pleistocene Artifact Sites in Olduvai Gorge, Tanzania. *J. Anthropol. Archaeol.* **1994**, *13*, 228–254. [CrossRef]
32. Gruškovnjak, L. Surveying along the Slopes: Evaluating the Impact of Geomorphic Processes on Field Survey's Site Discovery Effectiveness. *J. Field Archaeol.* **2024**, *49*, 1–26. [CrossRef]
33. Ozán, I.L. Gravity and the formation of the archaeological record: Main concepts and methodological tools. *Geoarchaeology* **2017**, *32*, 646–661. [CrossRef]
34. Duo, E.; Fabbri, S.; Grottoli, E.; Ciavola, P. Uncertainty of Drone-Derived DEMs and Significance of Detected Morphodynamics in Artificially Scraped Dunes. *Remote Sens.* **2021**, *13*, 1823. [CrossRef]
35. Zimmerman, T.; Jansen, K.; Miller, J. Analysis of UAS Flight Altitude and Ground Control Point Parameters on DEM Accuracy along a Complex, Developed Coastline. *Remote Sens.* **2020**, *12*, 2305. [CrossRef]

36. Rouse, L.M.; Krumnow, J. On the fly: Strategies for UAV-based archaeological survey in mountainous areas of Central Asia and their implications for landscape research. *J. Archaeol. Sci. Rep.* **2020**, *30*, 102275. [CrossRef]
37. Liu, X.; Lian, X.; Yang, W.; Wang, F.; Han, Y.; Zhang, Y. Accuracy Assessment of a UAV Direct Georeferencing Method and Impact of the Configuration of Ground Control Points. *Drones* **2022**, *6*, 30. [CrossRef]
38. Field, S.; Waite, M.; Wandsnider, L. The utility of UAVs for archaeological surface survey: A comparative study. *J. Archaeol. Sci.-Rep.* **2017**, *13*, 577–582. [CrossRef]
39. Agapiou, A.; Vionis, A.; Papantoniou, G. Detection of Archaeological Surface Ceramics Using Deep Learning Image-Based Methods and Very High-Resolution UAV Imageries. *Land* **2021**, *10*, 1365. [CrossRef]